Results in Physics 3 (2013) 84–90

Contents lists available at SciVerse ScienceDirect

Results in Physics

journal homepage: www.journals.elsevier.com/results-in-physics

Nonlinearity exponent in low dimensional nanotubes and nanowires

U.N. Nandi [a,*], Y.Z. Long [b,*], D. Chakraborty [a,c]

[a] Department of Physics, Scottish Church College, 1 & 3 Urquhart Square, Kolkata 700 006, India
[b] College of Physics, Qingdao University, Qingdao 266071, People's Republic of China
[c] Department of Physics, University of Calcutta, 92 A.P.C. Road, Kolkata 700 009, W.B., India

ARTICLE INFO

Article history:
Received 26 January 2013
Accepted 20 May 2013
Available online 31 May 2013

Keywords:
Nanowires/nanotubes
Conductance
Non-Ohmic
Nonlinearity exponent
Scaling
Tunneling

ABSTRACT

A scaling formalism is used to analyze non-Ohmic conductance-voltage data in nanowires of an isolated potassium manganese oxide $K_{0.27}MnO_2{\cdot}0.5H_2O$ and a poly(3,4-ethylenedioxythiophene) (PEDOT) and nanotubes of conducting polypyrrole at different temperatures. This scaling analysis provides a single voltage scale for non-Ohmic conduction which scales with Ohmic conductance with an exponent x_T, called nonlinearity exponent. A detailed analysis reveals that the onset exponents x_T are different in different systems. Non-Ohmic conduction and the nonlinearity exponents in these low-dimensional nanostructures are analyzed within the framework of scaling approach and existing theoretical models.

1. Introduction

Quasi-one-dimensional nanostructures such as nanotubes [1–7], nanowires [6–9], and nanofibres [3–5,10] are being studied extensively due to their importance in fundamental research and potential applications in nanoscale devices [11,12]. These systems are widely used as sensors in molecular electronics [13], as field effect transistors in nanoelectronics [14,15] and as chemical and bio-sensors in bio-nanotechnology and medicine [16]. These low-dimensional materials especially nanowires and nanotubes are prepared with chemical doping and are known to possess structural inhomogeneity having ordered conduction regions separated by small insulating barriers. This complex micro-structure of the low dimensional systems affects the various physical properties in particular the electrical transport [17,18]. In order to explore the salient features of the electrical transport and their possible applications, a number of experimental [4,6,7] and theoretical [19–22] studies have been made in these low dimensional nanostructures. However, its systematic description mainly in the non-Ohmic region is still lacking.

In low-dimensional systems, several physical properties show interesting behavior in contrast to their bulk counterpart. For example, electrical conductivity [23] and elastic constants [24] increase sharply with the decrease in diameter of the conducting polymer nanowires and nanotubes, and magneto-resistance of isolated polymer nanowires/tubes at low-temperatures is much smaller than that of the bulk pellets or films [25]. A number of conduction mechanisms such as variable range hopping due to Mott (M-VRH) [19] and its modification by Efros and Shklovskii (ES-VRH) [22] in the presence of coulomb interaction and fluctuation induced tunneling (FIT) due to Sheng et al. [20] have been considered to describe the electrical transport behavior in the low-dimensional materials [6,16,26,27] at low field strengths. In M-VRH model, an electron near the Fermi level hops between localized states separated by certain physical distances and having energy differences by absorbing phonons. The Ohmic conductance Σ_0 is obtained by optimizing the electron hopping paths using the relation:

$$\Sigma_0(T) = \Sigma_m \exp\left[-\left(\frac{T_0}{T}\right)^m\right] \quad (1)$$

Here Σ_m is the conductance pre-factor. T is the temperature and the exponent is $m = 1/(d+1)$ with d is the dimensionality of the system under consideration. The characteristic temperature T_0 is given by $T_0 = 4\pi/3N(E_F)K_Ba^3$ where $N(E_F)$ is the density of states at the Fermi level, K_B is the Boltzmann constant and a is the localization length. The conduction behavior at low field strengths in three as well as two dimensional systems is well described by this M-VRH model.

* Corresponding authors. Tel.: +91 033 2350 3862; fax: +91 033 2350 5207.
E-mail addresses: un_nandi@yahoo.co.in (U.N. Nandi), yunze.long@163.com (Y.Z. Long).

2211-3797
http://dx.doi.org/10.1016/j.rinp.2013.05.003

p-toluensulfonate (PTS)-doped PPy films [28] are reported to yield $m = 1/3$ suggesting two-dimensional nature. The exponent m in single crystals of PTS-doped polydiacetylene (PDA) [29] is found to be ~0.65–0.70 apparently demonstrating quasi-one dimensional nature of the system. In ES-VRH model [22], electron–electron interaction opens up a coulomb gap in the density of states at the Fermi level and the value of m becomes 1/2 which is independent of d. In this model, T_0 is given by

$$T_0 = \frac{2.8e^2}{4\pi\epsilon_0\epsilon K_B a}, \tag{2}$$

where ϵ is the dielectric constant. PEDOT [30] and Polypyrrole (PPy) films [31] tend to follow ES-VRH particularly at low temperatures with $m = 1/2$.

Non-Ohmic conduction is a common feature of the low-dimensional nanotubes and nanowires [6,16,26,27]. For small applied voltage V, the conductance $\Sigma(V)$ at a fixed temperature remains almost constant to its zero-voltage Ohmic value Σ_0. However with an increase in V, $\Sigma(V)$ increases from Σ_0 showing the non-Ohmic characteristics. The value of V at which $\Sigma(V)$ deviates from Σ_0 for the first time is known as the onset voltage V_0 and the corresponding current is known as the onset current I_0 [32]. Such non-Ohmic conduction has been observed in films [32], composites [33], conducting polymers [34] and manganites [35,37]. This common feature of the non-Ohmic conduction in different types of disordered systems is expressed using the scaling relation [34–37]:

$$\frac{\Sigma(V)}{\Sigma_0} = g\left(\frac{V}{V_0}\right), \tag{3}$$

where $g\left(\frac{V}{V_0}\right)$ is a scaling function. For $V \leqslant V_0$, $g\left(\frac{V}{V_0}\right) \approx 1$ and this corresponds to the fact that the conductance remains almost constant to Σ_0. At voltages $V \geqslant V_0$, $g\left(\frac{V}{V_0}\right) \geqslant 1$. Thus, the voltage V_0 at a fixed temperature separates the Ohmic regime from the non-Ohmic regime along the voltage axis. It has been shown by several authors that the scaling description given by Eq. (3) is applicable to various disordered systems like amorphous and doped semiconductors [34], films [34], composites [33,36], conducting polymers [34] and lightly doped manganites [35,37]. This onset voltage V_0 scales with zero-voltage Ohmic conductance Σ_0 [34–36] as

$$V_0 = A_T\ \Sigma_0^{x_T}, \tag{4}$$

where A_T is a constant. The value of A_T is determined by fixing the voltage scale V_0. x_T is the nonlinearity exponent, also known as the onset exponent. It has been shown in Refs. [34,35] that T does not enter *explicitly* in Eq. (3) but does so through the parameter Σ_0 which depends on temperature. Thus, the voltage scale V_0 for nonlinearity is determined solely by the Ohmic conductance Σ_0. Experimental results [34,35,37] show that disordered systems possess a single voltage scale V_0 and the non-Ohmic conduction takes place upon the application of only a few volts across the samples. Similar scaling description of ac conductance has been recently observed by Nandi et al. [38] in various disordered systems.

Several theoretical models such as variable range hopping under field [39], extended fluctuation induced tunneling (FIT) [20,40] and multi-step tunneling through n-localized states due to Glazman and Matveev (GM) [21] have been widely used for the analysis of non-Ohmic conduction in disordered systems. M-VRH is basically a zero voltage model to provide the conductance of disordered systems through hopping via localized states. At finite electric field, the accessible states are aligned to the occupied states allowing charge carriers to move along the field via phonon-assisted hopping. With further increase in field, the number of the aligned states increases near the onset field F_0 and the conductivity increases. At higher electric field strengths F, the energy eFR_h gained by an electron may become comparable to K_BT and leads to deviation from Ohmic behavior. R_h is the mean hopping length and e is the electronic charge. Theories [41,42] predict two characteristic field scales F_l and F_u corresponding to hopping and localization lengths respectively such that the non-Ohmic conductivity at intermediate field strengths $F < K_BT/e\ a$ is given by

$$\sigma(T,F) = \sigma(T,0)\ \exp\left(\frac{eFL}{K_BT}\right). \tag{5}$$

$\sigma(T,0) = \sigma_0$ is the Ohmic conductivity and L is a length related to the hopping length R_h. Clearly, the field $F_l = K_BT/eL$ could be identified as the onset field scale F_0 as discussed above. In the limit of large field strengths $F \geqslant K_B\ T/ea$, theories [42] agree with 'activationless' hopping at least qualitatively. In such situation the energy gained by an electron is large enough to hop without absorbing any phonons. As a result, the conductivity becomes independent of temperature and is given by

$$\sigma \sim \exp\left[-\left(\frac{F_u}{F}\right)^m\right],\ \text{where } F_u = \lambda\frac{K_BT_0}{ea}. \tag{6}$$

Here m and T_0 are same as in Eq. (1). λ is a numerical constant equal to unity [42] when $m = 1/4$.

Glazmann and Matveev [21] considered the process of multi-step indirect tunneling through n-localized states in a disordered system and proposed the following expression for conductance through tunnel barriers of an amorphous material under external bias V ($eV \gg K_BT$, $p_n = n - 2/(n+1)$):

$$\Sigma = \Sigma_d + \sum_1^n \Sigma_n V^{p_n} = \Sigma_0 + \Sigma_2 V^{1.33} + \Sigma_3 V^{2.5} + \Sigma_4 V^{3.6} + \Sigma_5 V^{4.67} + \Sigma_6 V^{5.71} + \ldots,. \tag{7}$$

Here $\Sigma_0 = \Sigma_d + \Sigma_1$. Σ_d accounts for the direct tunneling and Σ_1 for the elastic resonant tunneling via one localized state. Each term (for $n > 1$) in the series arises out of the events when a number of localized states happen to be arranged physically as well as energetically in such a way that an electron can traverse a sample length via multi-step inelastic tunneling. Each term may be said to constitute a separate channel of conduction. Thus, the macroscopic nonlinearity in this GM-model results from two contributions: appearance of new channels with increasing bias and nonlinearity of each such channel. This multi-step tunneling model has been widely used to explain relevant data in various tunnel junctions [43], lightly doped conducting polymer [34], and manganites [35,44,45]. Following the procedure adopted by Talukdar et al. [34], Eq. (7) can be made compatible with the scaling given in Eq. (3) by assuming that for $n \geqslant 2$, the coefficients satisfy the following relation

$$\Sigma_n = c_n\Sigma_0 V_0^{-p_n}. \tag{8}$$

Here c_n are constants and can be determined if coefficients Σ_n and onset voltage V_0 are known. Using this expression, Eq. (7) can be written as

$$\frac{\Sigma}{\Sigma_0} = 1 + c_2\left(\frac{V}{V_0}\right)^{1.33} + c_3\left(\frac{V}{V_0}\right)^{2.5} + c_4\left(\frac{V}{V_0}\right)^{3.6} + c_5\left(\frac{V}{V_0}\right)^{4.67} + c_6\left(\frac{V}{V_0}\right)^{5.71} + \ldots \tag{9}$$

Eq. (9) is thus really a scaling function and implies the existence of a single bias scale V_0 as in Eq. (3).

In this report, the experimental results of electrical transport in a number of low-dimensional nanowires and nanotubes over a wide range of temperatures are presented both in Ohmic and non-Ohmic regimes. Attempts are made to test the validity of the scaling function $g(y)$ given by Eq. (3) and to extract the onset exponents x_T defined in Eq. (4). Attention is also paid to find the nature

of the voltage dependence of the conductance both at Ohmic and Non-Ohmic regimes. Experimental details are given in Section 2. In Section 3, the data are presented, analyzed and discussed by scaling approach. Finally, we conclude the results in Section 4.

2. Experiments

Crystalline nanowires of $K_{0.27}MnO_2{\cdot}0.5H_2O$ were synthesized by the hydrothermal method. Analytical grade $KMnO_4$, $MnCl_2$ and KOH were obtained from Shanghai Chemical Co., and used without further purification. In a typical synthesis procedure, 1 mmol $KMnO_4$ and 1.5 mmol $MnCl_2$ were dissolved in 50 ml deionized water, then 40 g KOH was added into the solution under drastic stirring as a mineralizer. Finally, the solution was poured into a 100 ml Teflon vessel, sealed in a stainless steel autoclave, and maintained at 265 °C for 10 h under autogenous pressure. After the autoclave was cooled to room temperature, the final product was filtered off and washed sequentially with deionized water and absolute ethanol, then dried in ambient air at 60 °C for 2 h. More details can be found in [26,25]. Scanning electron microscopy (SEM) images of the nanowires shows that the diameter of the resulting nanowires is about 50–200 nm, and the length can be up to hundreds of micrometers [25]. Polypyrrole (PPy) nanotubes used in this work were prepared by using the typical template-free self-assembly method [6,27]. Pyrrole monomer (0.002 mol) and p-toluene sulfonic acid (PTSA, 0.001 mol) were mixed as dopant in 10 ml of distilled water. The mixture reacted and formed a transparent solution of PTSA–pyrrole salt and was cooled in an ice bath. Then an aqueous solution of ammonium persulphate (0.002 mol in 5 ml of distilled water) cooled in advance was added slowly into the PTSA–pyrrole salt solution. After reacting for 15 h in the ice bath, the precipitate was filtered out from the solution and washed sequentially with distilled water, ethanol, and ether several times. Finally the solution was dried for 24 h at room temperature in dynamic vacuum. PEDOT nanowires with a diameter of about 92 nm were prepared by using the template method according to a typical synthesis procedure as in Ref. [27].

Two Pt microleads in a $K_{0.27}MnO_2{\cdot}0.5H_2O$ nanowire and four Pt microleads in PPy nanotube and PEDOT nanowires were fabricated by the focused-ion beam deposition technique (Dual-Beam 235 Focussed-Ion Beam System from FEI Company; the working voltage of the system was 30 kV and the focused-ion beam current was 10 pA). The current–voltage (I–V) characteristics of nanostructured samples were measured by using a Physical Property Measurement System from Quantum Design and a Keithley 6487 picoammeter/voltage source over a wide temperature range from 300 to 20 K. The I–V curves were obtained by scanning the voltage from −2 V to 2 V in steps of 0.02 V for the single $K_{0.27}MnO_2{\cdot}0.5H_2O$ nanowire and from −5 V to 5 V in steps of 0.005 V for PPy nanotube and PEDOT nanowire samples.

3. Results and discussion

Fig. 1 shows the variation of zero-voltage Ohmic conductance Σ_0 with temperature of four samples: $K_{0.27}MnO_2{\cdot}0.5H_2O$ nanowire of diameter 148 nm, PPy nanotube of diameter 160 nm, PPy-HQSA nanotube and PEDOT nanowire. The Ohmic conductance data of PPy-HQSA nanotube and PEDOT nanowire are multiplied by 10 to show them separately in the figure. The solid lines are fits to Σ_0–T data of all the samples with the variable range hopping given by the Efros–Shklovskii (ES) law: $ln\Sigma_0 \sim T^{-1/2}$. These fits are extended over several orders of magnitude of Ohmic conductances Σ_0, e.g. three orders of magnitude in $K_{0.27}MnO_2{\cdot}0.5H_2O$ nanowire and five orders of magnitude in PPy nanotube. Excellent linearity of the fits to each curve indicates that within the measured range

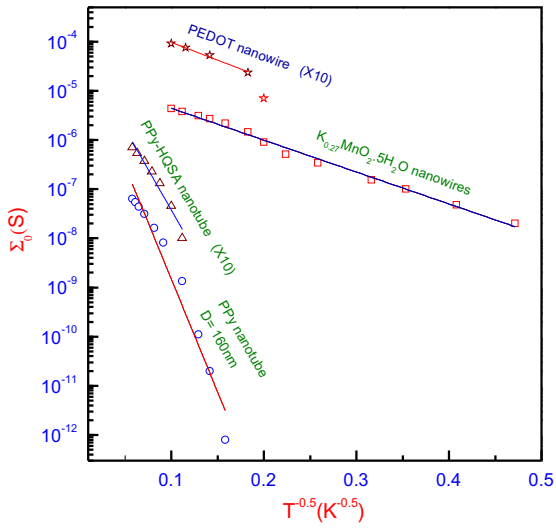

Fig. 1. Variation of zero-voltage dc conductance as a function of temperature T for four different samples of nanostructured systems. For clarity, the data of PPy-HQSA nanotube and PEDOT nanowire have been shifted upward by a factor of 10. Solid lines are linear fits to the data.

of temperature all the samples obey ES-type variable range hopping conduction.

The voltage dependence of conductance of a $K_{0.27}MnO_2{\cdot}0.5H_2O$ nanowire of diameter 148 nm and a PPy nanotube of diameter 160 nm are shown in Fig. 2(a) and (b) respectively in log–log scales. Linear conductances Σ_0 of both the samples were varied by varying temperature T at a fixed disorder D. The temperatures at which the $\Sigma(V)$–V data were taken are mentioned in the figures. The non-Ohmic response of conductance to the applied voltage can be seen in both the figures. At a constant temperature of 100 K, the conductance of the $K_{0.27}MnO_2{\cdot}0.5H_2O$ nanowire remains constant to its zero-voltage Ohmic value Σ_0 up to the onset voltage V_0. With further increase in voltage beyond V_0, the conductance increases monotonically indicating non-Ohmic behavior as a function of V. Qualitatively similar non-Ohmic transport behavior of conductance with voltage was also observed at other temperatures. Ohmic conductance Σ_0 decreases with decreasing T following the ES law [39] and the sample at low T becomes non-Ohmic at a smaller voltage i.e. V_0 *decreases* with decreasing temperature upto the measured range of temperature. This is clearly seen by the orientation of the dotted line in the Fig. 2(a). All $\Sigma(V)$–V curves corresponding to different temperatures approach each other at higher voltages. Similar features of non-Ohmic response of the conductance to the applied voltage V at different temperatures were also observed in PPy nanotube (diameter 160 nm) as shown in Fig. 2(b). Onset voltage V_0 increases with the increase in T as shown by the orientation of the dotted line. The $\Sigma(V)$–V curves at different temperatures in this nanotube also approach each other at higher voltages.

The panels (a), (b), (c) and (d) of Fig. 3 show the results of different $\Sigma(V)$–V data collapse into a master curve by data collapse method. The scaled data of the panels (a) and (c) correspond to the $\Sigma(V)$–V data of the Fig. 2(a) and (b) respectively. The data collapse method for obtaining the master curve is discussed in detail for $K_{0.27}MnO_2{\cdot}0.5H_2O$ nanowire system. The $\Sigma(V)$ –V curve at 100 K is considered appropriate for starting the scaling as the conductance possesses predominantly Ohmic and minimum non-Ohmic regime. The conductance at 100 K was divided by its Ohmic value Σ_0 and the voltage is kept unaltered (i.e. divided by 1). This value (=1) of voltage is considered as the onset voltage V_0 corresponding to the temperature 100 K. In fact for the first $\Sigma(V)$–V curve at a

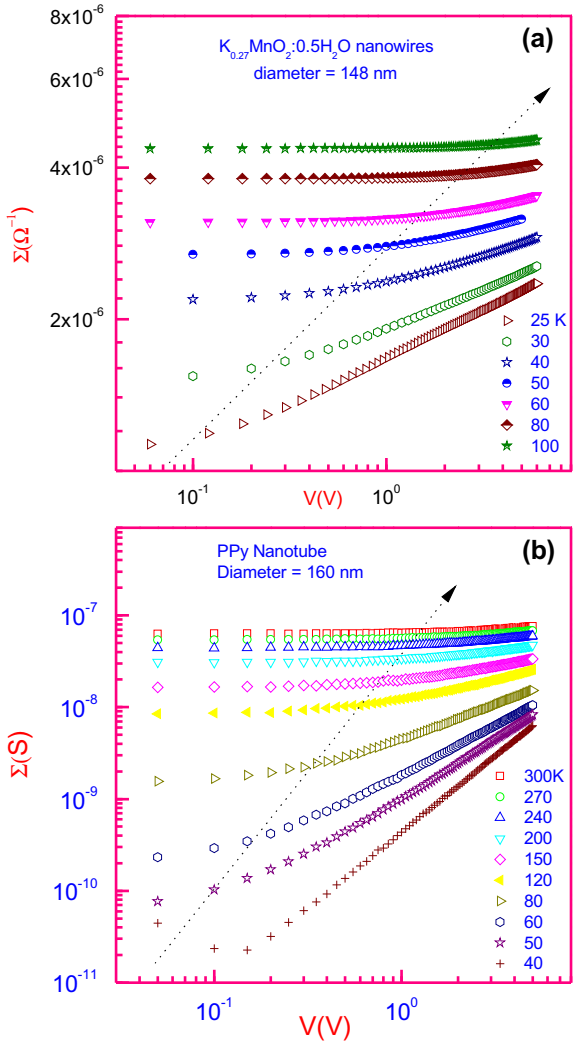

Fig. 2. (a) Variation of conductance vs. voltage in a sample of $K_{0.27}MnO_2$·0.5H_2O nanowire of diameter 148 nm at different temperatures as indicated. The dashed line schematically indicates the movement of the onset voltage with increasing temperatures. (b) Similar data as in (a) taken in a sample of polypyrrole nanotube of diameter 160 nm at different temperatures mentioned in the figure. The dashed line schematically indicates the movement of the onset bias with increasing temperatures.

particular temperature, any arbitrary choice for V_0 could be adapted as far as data collapse is concerned. For the next lower temperature (80 K), the conductance was divided by Σ_0 as before but the voltage was divided by a factor in such a way that this new set of data merged with the earlier one (corresponding to 100 K) as best as possible and this factor becomes the onset voltage V_0 at the temperature of 80 K. Notice that in this method V_0 is determined only up to a constant value. The same procedure was then repeated for the remaining $\Sigma(V)$–V curves corresponding to other temperatures in decreasing order. Such scaled conductance versus voltage data are shown in panel (a) of Fig. 3. The data collapse up to $\Sigma(V)/\Sigma_0 \approx 2.6$ seen in Fig. 3(a) proves the existence of a single voltage scale at each temperature. Conductance versus voltage data for the samples of PEDOT nanowire, PPy nanotube and PPy HQSA nanotube were scaled following the above mentioned procedure of data collapse and the scaled data are shown respectively in the panels (b), (c) and (d) of Fig. 3. The values of $\Sigma(V)/\Sigma_0$ for the systems are respectively 2, 10^4 and 10. These master curves indicate that the description of the non-Ohmic transport by the Eq. (3) is valid in low dimensional nanowires and nanotubes.

In the inset of the panel (a) of Fig. 3, V_0 obtained from the data collapse method corresponding to the $\Sigma(V)$–V curves of $K_{0.27}MnO_2$·0.5H_2O nanowire is shown in a log–log plot as a function of Σ_0. The solid line is a fit according to the expression: $V_0 \sim \Sigma_0^{x_T}$ with x_T being equal to 3.98 ± 0.104. Similar plots in the insets of the panels (b), (c) and (d) of Fig. 3 provide x_T equal to 2.94 ± 0.18, 0.88 ± 0.04 and 1.63 ± 0.041 respectively for PEDOT nanowire, PPy nanotube and PPy HQSA nanotube. The conductance corresponding to temperatures 40 K and 60 K for the PPy and PPy-HQSA nanotubes respectively is excluded in obtaining the nonlinearity exponent x_T as determination of conductance at these temperatures becomes unreliable due to fluctuation. These values of x_T are shown in column III of Table 1.

The last section dealt with the results of the variation of dc conductance as a function of voltage both in linear and nonlinear regimes in low-dimensional $K_{0.27}MnO_2$·0.5H_2O nanowire, PEDOT nanowire and PPy nanotube. The fibril chain-like constituents [5] make these systems structurally inhomogeneous. These polymeric chains are ordered in some regions, and disordered in some other regions. This complex structure consists of long conducting pathways separated by small insulating barriers. Electrons in the conduction regions interact through Coulomb repulsion and open up a soft gap in the density of localized states at the Fermi level resulting ES-VRH conduction as seen in Fig. 1. This interaction in nanostructures is enhanced due to the confinement of electrons and is almost 20–40 times larger than that for bulk samples [5]. At sufficiently low temperatures, the zero bias anomaly [25] and smooth crossover from M-VRH to ES-VRH [5] confirm that the Coulomb gap arising out of the electron–electron interaction indeed influences the hopping transport in the low-dimensional nanostructures. The diameter of the nanowires and nanotubes (of the order of 50–200 nm) is much larger than the localization length (less than 15 nm) of the electrons confirming the three-dimensional character of the system in regard to the motion of the electrons. This indicates that temperature dependence given by Eq. (1) with $m = 1/2$ is due to ES-VRH not the one-dimensional M-VRH.

The $\Sigma(V)$–V of $K_{0.27}MnO_2$·0.5H_2O nanowires and PPy nanotubes presented respectively in Fig. 2(a) and (b) are non-Ohmic i.e. conductance at a particular temperature is a function of voltage. Similar features of non-Ohmic behavior were also found in PEDOT nanowire and PPy-HQSA nanotube. This non-Ohmic conduction is characterized by a single voltage scale V_0 corresponding to each temperature. With decrease in temperature T, V_0 decreases which indicates that non-Ohmic conduction is enhanced at low T. Further the $\Sigma(V)$–V characteristics of all the systems under consideration at different T reveal a common feature that the increase in conductance $\Delta\Sigma(=\Sigma(V)-\Sigma_0)$ increases with decrease in T. Here $\Sigma(V)$ is the conductance at the highest voltage corresponding to a particular temperature. This $\Delta\Sigma$ is different in different systems in the same range of T. For example, $\Delta\Sigma$ is nearly three orders of magnitude in PPy nanotube but it is only a factor of two in $K_{0.27}MnO_2$·0.5H_2O nanowire. Different values of $\Delta\ \Sigma$ indicate the different degree of nonlinearity in different systems.

The non-Ohmic conduction in these nano-structured systems can be qualitatively understood in the following way: due to the presence of defects, nano-tubes and nano-wires do not tend to be single crystal over the whole length of the sample and can be viewed as an one-dimensional array of small crystalline grains separated by multiple tunneling junctions. At low bias, conduction occurs through these one-dimensional conducting arrays resulting Ohmic character of conductance. With the increase in bias, the rate of tunneling through these multiple tunnel junctions increases and as a result conductance also increases with voltage. As the temperature increases, electrons from different conducting regions start hopping giving larger conductance. The tunnel junctions of relatively larger separation start contributing in the conduction at

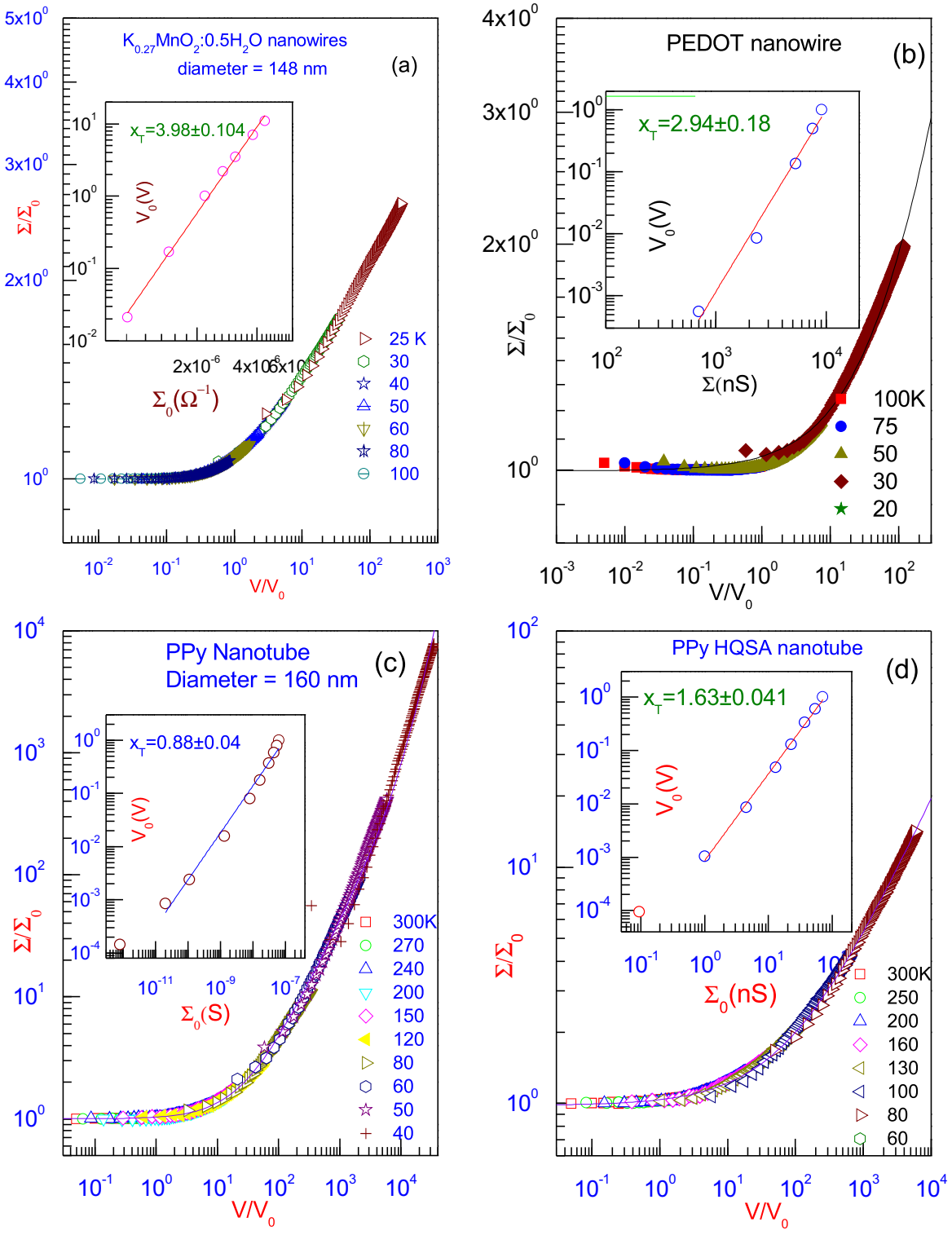

Fig. 3. Scaled conductance vs. scaled voltage plots of two samples of nanowires (a) $K_{0.27}MnO_2{\cdot}0.5H_2O$ and (b) PEDOT and two samples of nanotubes (c) Polypyrrole and (d) Polypyrrole HQSA. The solid lines in figures (b)–(d) are the fits according to the following expressions respectively: $\frac{\Sigma(V)}{\Sigma_0} = 0.998 + 0.0452 \times \left(\frac{V}{V_0}\right)^{0.66}$, $\frac{\Sigma(V)}{\Sigma_0} = 1 + 0.033 \times \left(\frac{V}{V_0}\right)^{1.03} + 4.5 \times 10^{-8} \times \left(\frac{V}{V_0}\right)^{2.48}$ and $\frac{\Sigma(V)}{\Sigma_0} = 0.98 + 0.056 \times \left(\frac{V}{V_0}\right)^{0.63}$. Insets in all the figures (a) –(d) show log–log plots of onset voltage $V_0(V)$ against linear conductance $\Sigma_0(S)$. The solid lines in figures (a)–(d) are the power-law fits to the data with the slopes x_T as indicated.

higher bias. This indicates that V_0 increases with T as pointed out by the orientation of the dotted lines in Fig. 2(a) and (b). Such non-Ohmic conduction has also been observed in several low-dimensional nanostructures e.g. p-toluensulfonate (PTS)-doped polydiacetylene (PDA) single crystal [29], individual iodine-doped polyacetylene nanofibre [40], Au-PPy-Au and Pt-PPy-Au nanowires [9], polyaniline nanotube [7], CdS nanorope [7], etc. PTS-doped PDA single crystals [29] are quasi-one-dimensional in nature, consisting of weakly coupled linear parallel chains of covalently bonded carbon atoms and obey VRH conduction with $m = 1/2$. The non-Ohmic behavior of conductivity in this system was also found to be enhanced with the lowering of temperature. Individual

Table 1
Onset exponents x_T for nonlinearity in dc conduction in various nanostructured systems. P stands for the variable used to vary Σ_0: T – Temperature.

Systems	P	x_T
$K_{0.27}MnO_2{\cdot}0.5H_2O$ nanowire of diameter 148 nm	T	3.98 ± 0.104
PEDOT nanowire of diameter 95 nm	T	2.94 ± 0.18
PEDOT nanowire of diameter 92 nm	T	2.85 ± 0.096
PPy nanotubes of diameter 160 nm	T	0.88 ± 0.04
PPy-HQSA nanotube	T	1.63 ± 0.041
PDA single crystal [34]	T	0.51 ± 0.02
Polianiline nanofibre [34]	T	0.33 ± 0.02

iodine-doped polyacetylene nanofibre [40] follows activated-type conduction at high temperatures but Zener-type tunneling at low temperatures. This system also shows nonlinear conductance characteristics at different temperatures. Gence et al. [9] observed electrical nonlinearity in Au-PPy-Au and Pt-PPy-Au nanowires in the temperature range from room temperature down to 0.5 K. The low temperature zero-voltage conductance data of the single nanowire of diameter 70 nm and multi-nanowire samples embedded in polycarbonate were described by 3 d M-VRH conduction mechanism [9]. The nonlinearity in these systems was successfully explained by the hopping relations given by Eqs. (5) and (6) respectively in the intermediate and high field strengths signifying the existence of two field scales in the systems corresponding to hopping and localization lengths.

The panels (a), (b), (c) and (d) of Fig. 3 indicate that the $\Sigma(V)$–V data of these nanostructured systems at different temperatures do indeed collapse into a master curve. The maximum value of the normalized conductance $\Sigma(V)/\Sigma_0$ varies from system to system: by a factor of two in $K_{0.27}MnO_2{\cdot}0.5H_2O$ nanowire and PEDOT nanowire, four orders of magnitude in PPy nanotube and one order of magnitude in PPy-HQSA nanotube. But the normalized voltage V/V_0 is extended over at least five orders of magnitude. This does signify that the description of non-Ohmic conduction by the scaling function (3) is valid in these nanostructured systems. Scaled conductance versus scaled voltage data shown in Fig. 3(b), (c) and (d) were fitted with the expression:

$$\frac{\Sigma(V)}{\Sigma_0} = 1 + c_1\left(\frac{V}{V_0}\right)^{\alpha_1} + c_2\left(\frac{V}{V_0}\right)^{\alpha_2} \tag{10}$$

where c_1, c_2, α_1 and α_2 are the fitting parameters. These parameters have values (0.0452, 0.0, 0.66 and 0.0), (0.033, 4.5×10^{-8}, 1.03 and 2.48) and (0.056, 0.0, 0.63 and 0.0) respectively for PEDOT nanowire, PPy nanotube and PPy-HQSA nanotube. The values of the parameters c's and α's are different in different systems. For example, α_1(=1.030) in PPy nanotube is much larger than in PEDOT nanowire ($\alpha_1 = 0.66$) and in PPy-HQSA ($\alpha_1 = 0.63$) nanotube signifying the fact that the electron–electron interaction in this nanotube is much stronger than the other two systems. α_2(=2.48) in PPy nanotube is very close to the power of the third term (=2.50) of the GM expression given in Eq. (9). This indicates that at higher voltages, the conduction channels mainly consist of three localized states. With the increase in voltage, these channels increase in number and provide paths for the flow of current causing the non-Ohmic conduction. These facts reflect that at lower voltages, the electron–electron interaction is prominent whereas at higher voltages three-step tunneling dominates the non-Ohmic conduction. The smaller value of the coefficient c_2(=4.5×10^{-8}) indicates that the number of such three-step channels is small. Within the measured range of voltages, the second term of Eq. (10) is not required while fitting the scaled conductance versus voltage data of PEDOT nanowire and PPy-HQSA nanotube. This indicates that multi-step tunneling has no contribution to conductance in these two systems and the increase in normalized conductance is small as observed in the scaled plots shown in the panels (b) and (d) of Fig. 3. But in PPy nanotube, the multi-step tunneling is operative at higher voltages indicating huge ($\sim10^4$) increase in normalized conductance.

Insets of the panels (a), (b), (c) and (d) of Fig. 3 show the log–log plot of the onset voltages V_0 corresponding to each temperature against the Ohmic conductances Σ_0. Fits to the data with Eq. (4) provide the values of x_T which are all positive as shown in Table 1. This indicates that V_0 increases with temperature T in these nanowire and nanotube systems. Further it is observed that in nanowire systems, x_T is relatively higher compared to the value of x_T in nanotubes. This indicates that a sample of nanowire becomes non-Ohmic at a voltage higher than that required for a sample of nanotube of comparable conductance. The values of x_T for two samples of PEDOT nanowire of diameters 92 and 95 nm indicate that similar-sized PEDOT nanowires have similar values of x_T. Except in PPy nanotube of diameter 160 nm, the values of x_T were found to be large compared to the value in composites [32], lightly doped conducting polymers [34] and manganites [35,37]. This indicates that nanowires/nanotubes possess strong electrical nonlinearity. In lightly doped conducting polymer x_T was probed experimentally along different paths by varying conductance by several variables e.g. temperature T, disorder D and magnetic field B [34] and was found to be positive, negative or even zero. The values of x_T of two such systems like PTS-doped PDA single crystals and individual iodine doped polyacetylene nanofibre are shown in Table 1. These values of x_T were successfully explained by the model of multi-step tunneling via n-localized states introduced by Glazman and Matveev [21]. It should be mentioned here that all these nanowires/nanotubes possess a single voltage scale V_0 within the measured range of voltage and temperature. The existence of such a single voltage scale V_0 has also been experimentally verified by Talukdar et al. [34] in several lightly doped conducting polymers available in bulk, film and single crystal forms. This experimental observation is contrary to the theoretical prediction of two voltage scales [41,42,46] corresponding to hopping and localization lengths in disordered systems. The field dependent conductance data of the nanostructured systems are successfully described by tunneling mechanism influenced by electron–electron interaction through the multiple tunneling junctions.

4. Conclusion

A comprehensive quantitative description of the variation of conductance of low-dimensional nanotubes and nanowires is presented over the temperature range from room down to 20 K and voltage range up to 6 V. Within the measured range of temperature, Ohmic conductance follows ES-type variable range hopping signifying the influence of electron–electron interaction on the conduction mechanism. The $\Sigma(V)$–V curves were found to be non-Ohmic and properly described by a single voltage scale V_0 corresponding to each temperature. This onset voltage sets an intrinsic length scale which leads to the associated scaling properties of various electrical quantities. The onset exponents x_T are all positive and different in different systems indicating that the microscopic details play a significant role in setting the non-Ohmic conduction in these nanostructures. The phenomenology of scaling, existence of a single voltage scale and the nonlinearity exponent x_T need to be supported by proper theoretical understanding.

Acknowledgements

This work was supported by the Department of Science and Technology, Government of India through Major Research Project No: SR/S2/CMP-0054/2008. Prof. Y.Z. Long is thankful to the National Natural Science Foundation of China (Grant No: 11074138), the Taishan Scholars Program of Shandong Province,

and the Shandong Provincial Natural Science Foundation for Distinguished Young Scholars, China (Grant No: JQ201103).

References

[1] Kang N, Hu JS, Kong WJ, Lu L, Zhang DL, Pan ZW, et al. Phys Rev B 2002;66:241403.
[2] Park JG, Kim B, Lee SH, Park YW. Thin Solid Films 2003;438:118.
[3] Ma YJ, Zhou F, Lu L, Zhang Z. Solid State Commun 2004;130:313.
[4] Aleshin AN, Lee HJ, Jhang SH, Kim HS, Akagi K, Park YW. Phys Rev B 2005;72:153202.
[5] Long YZ, Zhang LJ, Chen ZJ, Huang K, Yang YS, Xiao HM, et al. Phys Rev B 2005;71:165412.
[6] Long YZ, Yin ZH, Li MM, Gu CZ, Duvail JL, Jin AZ, et al. Chin Phys B 2009;18:2514.
[7] Yin ZH, Long YZ, Gu CZ, Wan MX, Duvail JL. Nanoscale Res Lett 2009;4:63.
[8] Samitsu S, Iida T, Fujimori M, Heike S, Hashizume T, Shimomura T, et al. Synth Met 2005;152:497.
[9] Gence L, Faniel S, Gustin C, Melinte S, Bayot V, Callegari V, et al. Phys Rev B 2007;76:115415.
[10] Park JG, Kim B, Lee SH, Kaiser AB, Roth S, Park YW. Synth Met 2003;135:299.
[11] MacDiarmid AG. Rev Mod Phys 2001;73:701.
[12] Aleshin AN. Adv Mater 2006;18:17.
[13] Cui Y, Wei Q, Park H, Lieber CM. Science 2001;293:1289.
[14] Cui Y, Lieber CM. Science 2001;291:851.
[15] Chung HJ, Jung HH, Cho YS, Lee S, Ha JH, Choi JH, et al. Appl Phys Lett 2005;86:213113.
[16] Long YZ, Li MM, Gu CZ, Wan M, Duvail JL, Liu Z, et al. Prog Polym Sci 2011;36:1415.
[17] Martin CR. Acc Chem Res 1995;28:61.
[18] Delvaux M, Duchet J, Stavaux PY, Legras R, Demoustier-Champagune S. Synth Met 2000;113:275.
[19] Mott NF. J Non-Cryst Solids 1968;8:1;
Mott NF. Philos Mag 1969;19:835.
[20] Sheng P, Sichel EK, Gittleman JL. Phys Rev Lett 1978;40:1197.
[21] Glazman LI, Matveev KA. JETP 1988;67:1276.
[22] Efros AL, Shklovskii BI. J Phys C 1975;8:49.
[23] Duvail JL, Long YZ, Cuenot S, Chen ZJ, Gu CZ. Appl Phys Lett 2007;90:102114.
[24] Cuenot S, Demoustier-Champagne S, Nysten B. Phys Rev Lett 2000;85:1690.
[25] Long YZ, Yin ZH, Chen ZJ, Jin AZ, Gu CZ, Zhang HT, et al. Nanotechnology 2008;19:215708.
[26] Zhang HT, Chen XH, Zhang JH, Wang GY, Zhang SY, Long YZ, et al. J Cryst Growth 2005;280:292.
[27] Long YZ, Chen ZJ, Shen JY, Zhang ZM, Zhang LJ, Huang K, et al. Nanotechnology 2006;17:5903;
Long YZ, Chen ZJ, Wang NL, Ma YJ, Zhang Z, Zhang LJ, et al. Appl Phys Lett 2003;83:1863;
Yang YS, Liu J, Wan MX. Nanotechnology 2002;13:771.
[28] Ribo JM, Anglada MC, Hernandez JM, Zhang X, Anglada NF, Chaibi A, et al. Synth Met 1998;97:229.
[29] Aleshin AN, Lee JY, Chu SW, Lee SW, Kim B, Ahn SJ, et al. Phys Rev B 2004;69:214203.
[30] Maji S, Mukhopadhyay S, Gangopadhyay R, De A. Phys Rev B 2007;75:073202.
[31] Bof Bufon CC, Heinzel T. Phys Rev B 2007;76:245206.
[32] Gefen Y, Shih W, Laibowitz RB, Viggiano JM. Phys Rev Lett 1986;57:3097;
Chakrabarty RK, Bardhan KK, Basu A. Phys Rev B 1991;44:6773;
Nandi UN, Bardhan KK. Europhys Lett 1995;31:101.
[33] Nandi UN, Bardhan KK, Mukherjee CD. Mater Sci Forum 1997;223–224:261.
[34] Talukdar D, Nandi UN, Bardhan KK, Bufon CC, Heinzel T, De A, et al. Phys Rev B 2011;84:054205.
[35] Ghosh TN, Nandi UN, Chattopadhyay S, Jana D, Saha SC. Solid State Commun 2012;152:1595.
[36] Jana D, Nandi UN. A statistical description of electrical transport in disordered systems. Saarbrucken, Germany: LAMBERT Academic Publishing GmbH and Co. KG; 2011.
[37] Talukdar D, Nandi UN, Poddar A, Mandal P, Bardhan KK. Phys Rev B 2012;86:165104.
[38] Nandi UN, Sircar S, Karmakar S, Giri S. J Phys Condens Matter 2012;24:265601.
[39] Mott NF, Davis EA. Electron processes in noncrystalline materials. 2nd ed. London: Clarendon Press Oxford; 1979.
[40] Kaiser AB, Rogers SA, Park YW. Mol Cryst Liq Cryst 2004;415:115.
[41] Hill RM. Philos Mag 1971;24:1307.
[42] Shklovskii BI. Sov Phys Semicond 1973;6:1964;
Shklovskii BI. Sov Phys Semicond 1976;10:855.
[43] Xu Y, Ephron D, Beasley MR. Phys Rev B 1995;52:2843.
[44] Hfener C, Philipp JB, Klein J, Alff L, Marx A, Bchner B, et al. Europhys Lett 2000;50:681.
[45] Markovich V, Jung G, Fita I, Mogilyansky D, Wu X, Wisniewski A, et al. J Mag Mag Mat 2010;322:1311.
[46] Pollak M, Riess I. J Phys C 1976;9:2339.